High-Reflectivity Heterovalent Distributed Bragg Reflectors for Infrared Resonant Cavity Applications

M.B. Lassise, B.D. Tracy, D.J. Smith, and Y.-H. Zhang
Arizona State University, Tempe, AZ 85281

Monolithically integrated midwave IR optoelectronic devices such as VCSELs, resonant-cavity LEDs and photodetectors are highly desirable for chemical sensing and environmental monitoring applications. One of the key components of these devices is the highly-reflective distributed Bragg reflector (DBR), which is comprised of a stack of alternating layers with different refractive indices designed to reflect a particular range of wavelengths. In this study, we first focus on ZnTe/GaSb DBRs, which have a high refractive index contrast ($\Delta n \approx 1$ for infrared wavelengths), similar lattice constants (lattice mismatch < 0.1%), and are epitaxially integrable with IR absorber materials like InAs/InAsSb, GaSb/InGaSb, InAsSbBi, and PbSe. Several DBR samples were grown using a single-chamber MBE system equipped with both II-VI and III-V source materials. The XRD pattern of a two-pair ZnTe/GaSb DBR is plotted together with the simulated results in Fig. 1. The grown structures demonstrate sharp interfaces and minimal interdiffusion between the heterovalent layers.

Fig. 2 shows the measured and simulated reflectance with a peak reflection value of approximately 98 % and a stopband width of about 70 meV centered on a wavelength of 4.5 μm for a 6 pair DBR. Fabry-Pérot cavities based on the DBRs are investigated to determine the viability of these structures for resonant-cavity devices. The reflectance spectra and minimum absorption levels of the DBR structures have been modeled using the transfer matrix formalism for a variety of material combinations lattice-matched to III-V substrates. Below-band gap losses such as free carrier absorption are calculated for short, mid, and longwave IR heterovalent DBR structures and compared with corresponding III-V DBRs. Additionally, the optical properties of resonant-cavity structures based on the heterovalent DBRs are simulated and the potential device characteristics, such as the cavity Q-factor, are compared for a range of cavity materials and operational wavelengths. Other lattice-matched heterovalent material combinations, such as ZnSe/GaAs and CdTe/InSb, are also under exploration for shortwave to longwave IR DBRs.

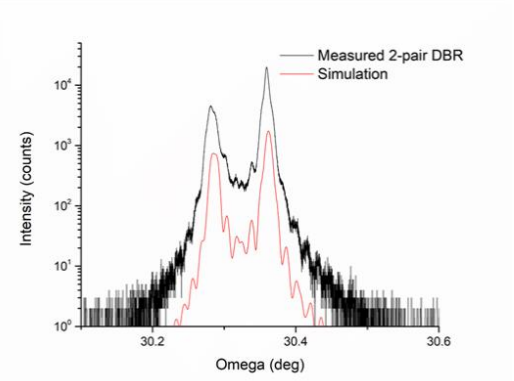

Figure 1: ω/2Θ X-ray diffraction spectrum of a dual-pair ZnTe/GaSb Bragg reflector sample.

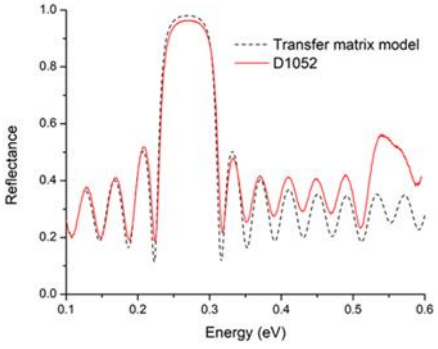

Figure 2: Measured reflection spectrum of a 6-pair ZnTe/GaSb DBR compared to the predicted reflectance.

+ Author for correspondence: mlassise@asu.edu

Supplementary Pages:

The grown sample structure for the ZnTe/GaSb DBRs is shown in Fig. 3. For growth on GaSb substrates, the oxide is removed at a substrate temperature of 540 °C with periodic Ga flashes before a 500 nm GaSb buffer is grown at 500 °C. After the buffer, an Sb flux is applied to the surface as the substrate cools to 350 °C before switching to a Zn flux as the temperature is further reduced to 300 °C. Zn-Sb bonding is promoted at the interface to avoid the formation of defective III-VI compounds. The ZnTe growth is initiated by opening the Te shutter once the substrate temperature hits 300 °C. The ZnTe is grown with a slight Te overpressure and a streaky 2×1 RHEED was observed. The Te shutter is closed to stop the ZnTe layer growth and the surface is exposed to a Zn flux until a c2×2 reconstruction is observed with RHEED. The surface is immediately flushed with a brief Sb soak once the Zn shutter is closed before starting the next GaSb layer. To maintain high-quality GaSb growth while limiting diffusion or desorption from the ZnTe layer, a temperature ramp is used to bring raise the substrate from 300 °C to 500 °C over a period of approximately 13 minutes. This process is repeated until the desired number of ZnTe/GaSb stacks is reached.

The reflectance of the DRB structures was measured using an FTIR blackbody source normalized to the spectrum of a gold mirror, and compared to calculations made by solving the Fresnel equations for normal angle incidence using the transfer matrix formalism, see Eq. 1 and 2. Chromatic dispersion in each material and the penetration depth were taken into account with the transfer matrix calculations. Free carrier absorption, a major impediment for LWIR dielectric mirrors, was calculated using Eq. 3 and 4 as a function of wavelength for heterovalent and isovalent material combinations, see Fig. 4. Optical cavity devices have been simulated by inserting a half-wavelength active layer between the DBRs, and an absorption peak FWHM of less than 2 meV was found for a target operation wavelength of 3 μm, shown in Fig. 5. Diffusion between the GaSb and ZnTe layers, which can lead to parasitic absorption as the unintentional dopants can create midgap trap states and increase the free carrier density, is quantified using SIMS and Hall measurements. Possible steps to limit diffusion between the materials, including reduction of the growth temperature and introduction of Al and Mg into the III-V and II-VI materials, respectively, will be discussed at the conference.

(1) $$\begin{bmatrix} A \\ B \end{bmatrix} = \left(\prod_m^{2N} \begin{bmatrix} Cos\left(\frac{2\pi n_m \cdot d_m}{\lambda}\right) & i \cdot Sin\left(\frac{2\pi n_m \cdot d_m}{\lambda}\right) \Big/ n_m \\ i \cdot n_m \cdot Sin\left(\frac{2\pi n_m \cdot d_m}{\lambda}\right) & Cos\left(\frac{2\pi n_m \cdot d_m}{\lambda}\right) \end{bmatrix} \right) \cdot \begin{bmatrix} 1 \\ n_{sub} \end{bmatrix}$$

(2) $$R(\lambda) = \left(\frac{1-\frac{B}{A}}{1+\frac{B}{A}}\right) \cdot \overline{\left(\frac{1-\frac{B}{A}}{1+\frac{B}{A}}\right)}$$

(3) $$\alpha_{FCA} = \frac{\sqrt{\varepsilon_0}\omega_p{}^2\lambda^2}{4\pi c^3 \tau}$$

(4) $$\omega_p = \sqrt{\frac{4\pi n q^2}{m^* \varepsilon_0}}$$

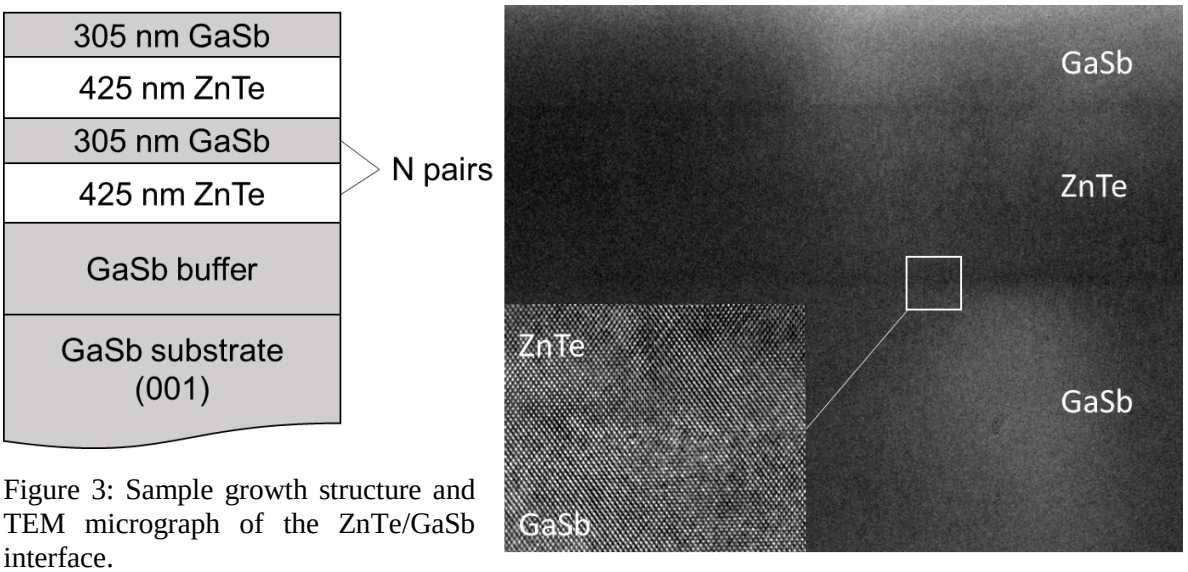

Figure 3: Sample growth structure and TEM micrograph of the ZnTe/GaSb interface.

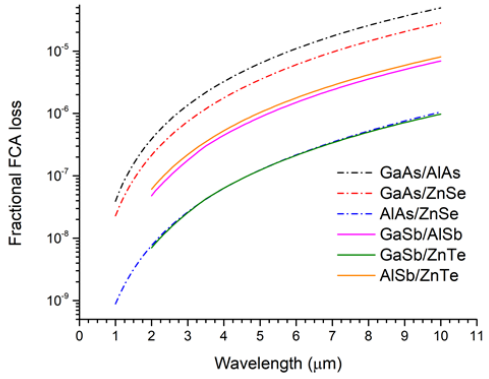

Figure 4: Calculated free carrier absorption as a function of wavelength for DBR structures closely lattice matched to GaAs (dashed lines) and GaSb (solid lines).

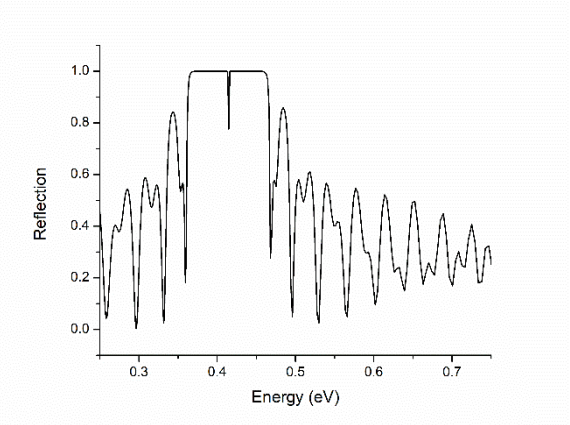

Figure 5: Simulated reflectance spectra of an InAs/$InAs_{0.85}Sb_{0.15}$ superlattice optical cavity confined by GaSb/ZnTe DBRs for precise detection/emission of the 3 μm wavelength.